

Supporting Information for

Core-shell ZnO/ZnFe₂O₄@C Mesoporous Nanospheres with Enhanced Lithium Storage Properties towards High-performance Li-ion Batteries

*Changzhou Yuan *, Hui Cao, Siqi Zhu, Hui Hua, Linrui Hou**

[*] *Prof. C. Z. Yuan, H. Cao, S. Q. Zhu, H. Hua, Prof. L. R. Hou*

School of Materials Science & Engineering, Anhui University of Technology, Ma'anshan, 243002,
PR China Email: ayuancz@163.com; houlr629@163.com

Prof. C. Yuan

Chinese Academy of Science (CAS) Key Laboratory of Materials for Energy Conversion, Hefei,
230026, P.R. China

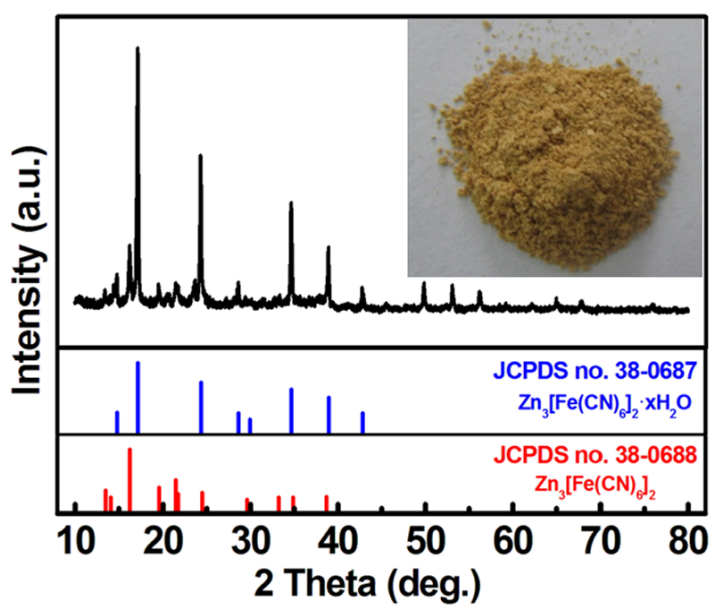


Fig. S1. Wide-angle XRD pattern and typical optical image (the inset) of the resulting ZFC

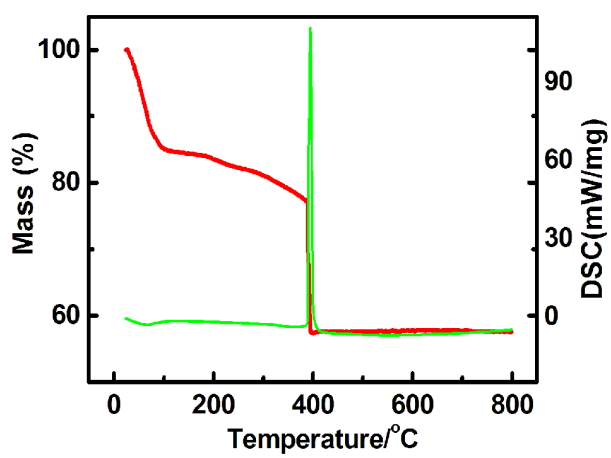


Fig. S2. TG data for the precursor of ZFC

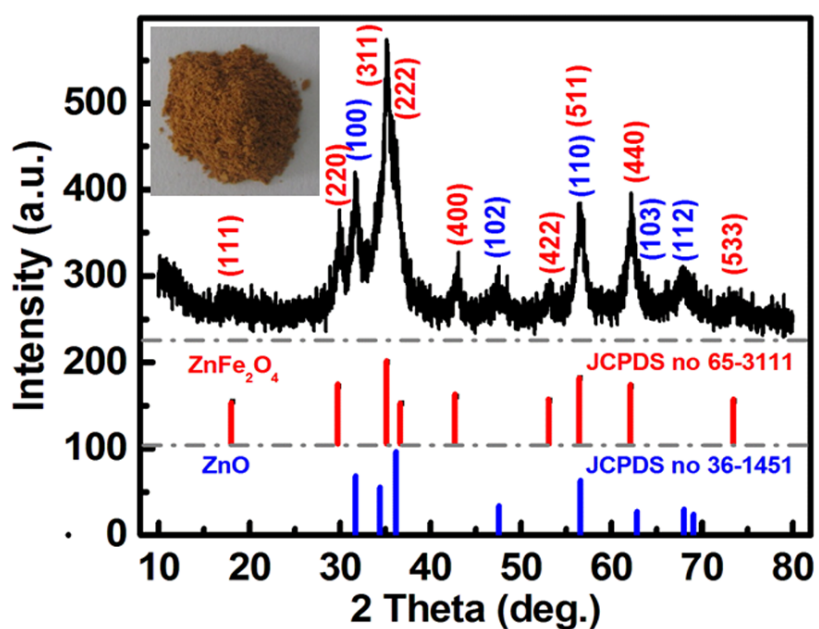


Fig. S3. Wide-angle XRD pattern and typical optical image (the inset) of the as-obtained ZZFO

Table S1 Atomic coordinates and occupation numbers for the ZFO in the ZZFO@C

Atom	Site	g	x	y	z
Zn	8a	1.4903	0	0	0
Fe	16d	1.3044	0.625	0.625	0.625
O	192i	1	0.16591	2.09577	-1.13885

Table S2 Atomic coordinates and occupation numbers for the ZnO in the ZZFO@C

Atom	Site	g	x	y	z
Zn	2b	0.9915	1/3	2/3	0
O	2b	1.1282	1/3	2/3	0.38314

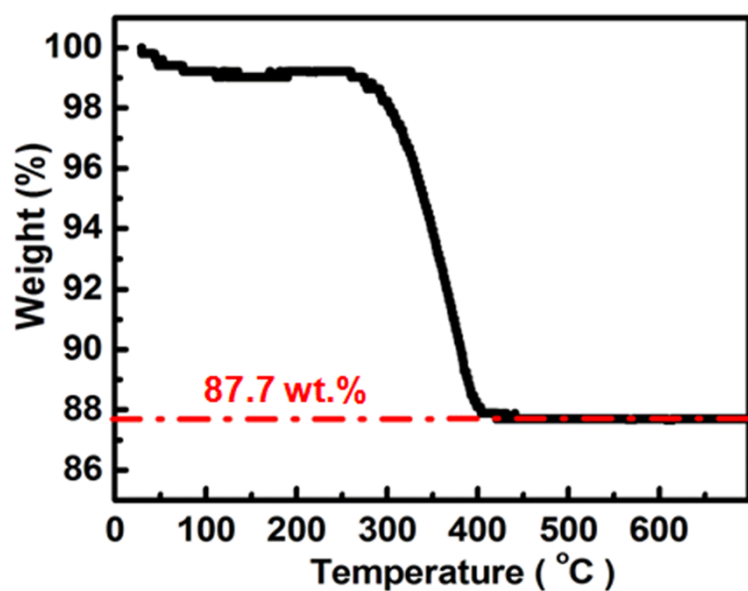


Fig. S4. TG analysis of the core-shell ZZFO@C under air flow with a temperature ramp of $10\text{ }^{\circ}\text{C min}^{-1}$

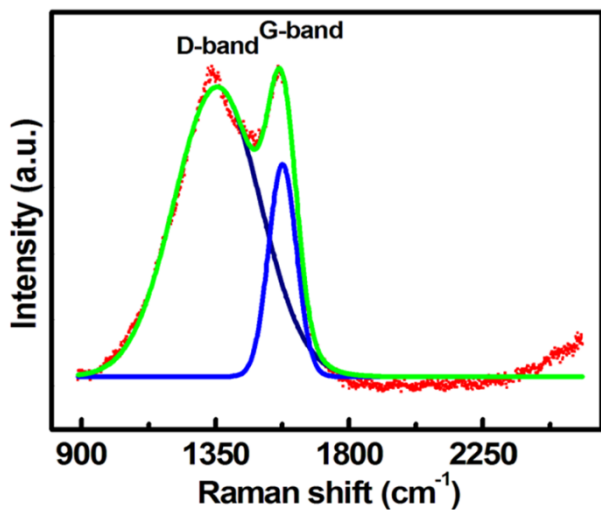


Fig. S5. Raman spectrum of the as-prepared core-shell ZZFO@C

To further verify the carbon species in the core-shell sample, corresponding Raman spectrum of the core-shell ZZFO@C from 888 to 2585 cm^{-1} is demonstrated in **Figure S5**. Two typical vibrational modes of carbonaceous materials, that is, the D-band centered at $\sim 1348 \text{ cm}^{-1}$ (A_{1g}) and the G-band sitting at $\sim 1567 \text{ cm}^{-1}$ (E_{2g}),^{1,2} are distinctly presented. And the intensity ratio of the D- to G-band is estimated as ~ 1.3 .

[1] L. Zhou, S. Q. Zhu, H. Cao, L. R. Hou, C. Z. Yuan, *Green Chem.*, 2015, **17**, 2373.

[2] L. R. Hou, L. Lian, D. K. Li, G. Pang, J. F. Li, X. G. Zhang, S. L. Xiong, S. L. Xiong, *Carbon*, 2013, **64**, 141.

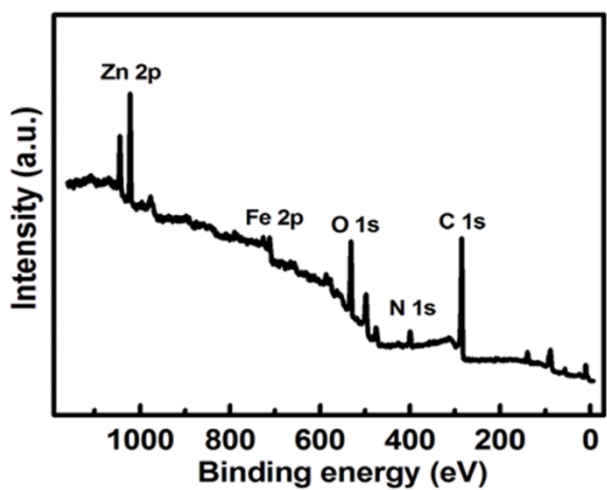


Fig. S6. Overview survey XPS spectrum of the as-prepared ZFC precursor

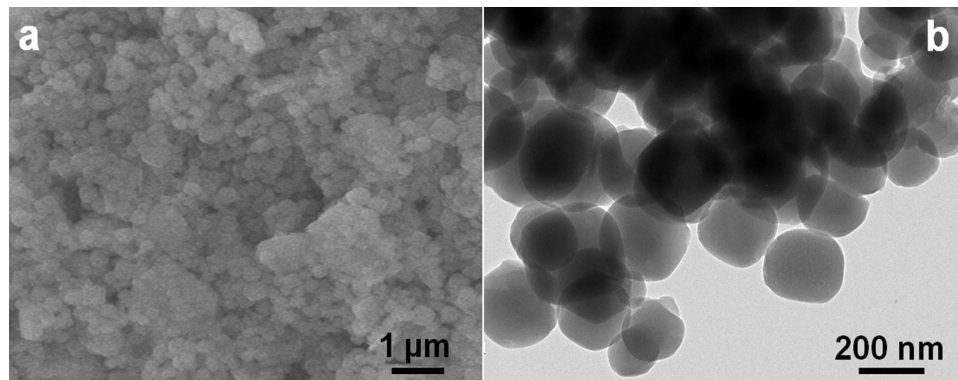


Fig. S7. FESEM (a) and TEM (b) images of the as-prepared ZFC precursor

The uniform-contrast TEM image of the nanospheres clearly confirms its solid nature.

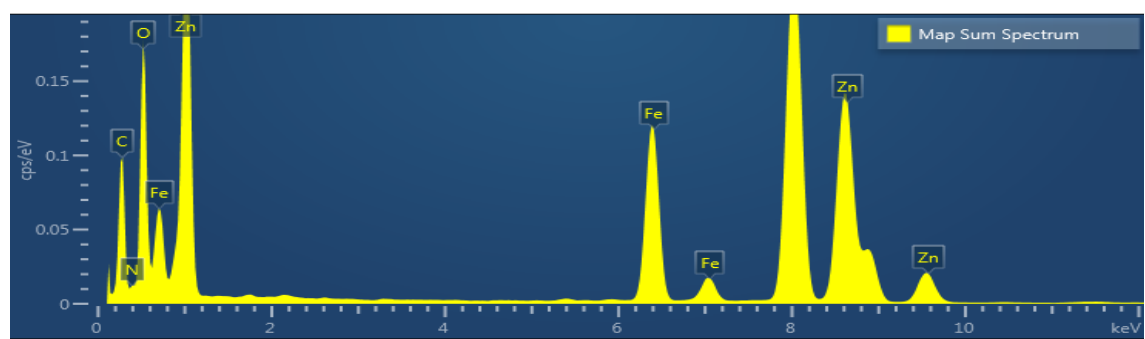


Fig. S8. EDXA spectrum of the as-synthesized core-shell ZZFO@C

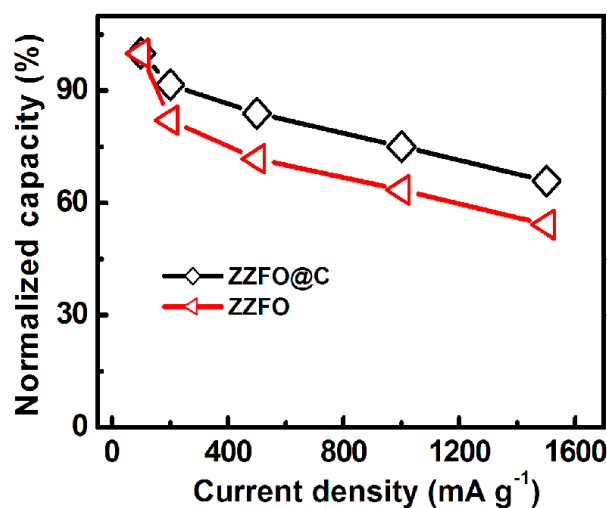


Fig. S9. Normalized capacity at each current step (Fig. 6c) by the average capacity under a current rate of 100 mA g⁻¹ of the initial step

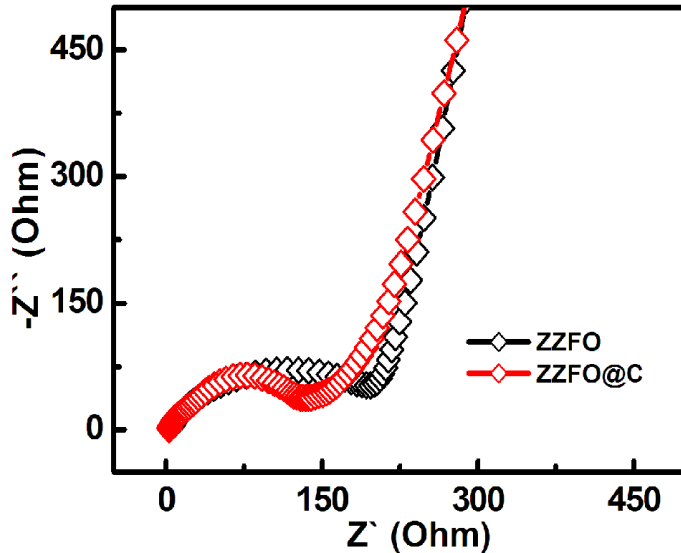


Fig. S10. EIS spectra of the ZZFO@C and ZZFO anodes at an open circuit voltage state using fresh cells as indicated

As seen from **Figure S9**, both of the two consist of a semicircle in the high to medium frequency region (100 – 10 kHz) and an inclined line in the low frequency range from (100 – 0.01 kHz). Of note, the diameter of high-frequency semicircle for the ZZFO@C anode is obviously smaller than that of the ZZFO, which indicates the smaller charge-transfer resistance (R_{CT}) of the fresh ZZFO@C. After fitted, the R_{CT} values are 287 and 176 Ohm, respectively, for the ZZFO and ZZFO@C. In addition, the intersections of these EIS plots with the X-axis, which represent solution resistance (R_s), including the resistance of the electrolyte itself, the intrinsic resistances of electroactive material itself and the contact resistance between electroactive material and current collector, are ~2.5 (ZZFO@C) and ~5.1 (ZZFO) Ohm for the two, as tabulated in **Table S4**.

Table S3 Initial Coulombic efficiency (CE) and cycling properties of the core-shell ZZFO@C anode in this study, compared with some other ZFO-based anodes reported in previous literature

Electrode materials	The 1 st CE (%)	Specific capacity ¹⁾ /cycle number/current density (mA g ⁻¹)	(mAh g ⁻¹)	Ref.
ZZFO@C	~76	~718/500/1000		This study
York-shell ZnFe ₂ O ₄	~74	~862/200/500		[1]
ZnFe ₂ O ₄ @C/graphene	~67	~712/232/50		[2]
ZnFe ₂ O ₄ -C composites	~81	~681/71/100		[3]
ZnFe ₂ O ₄ nano-fibers	~71	~733/30/60		[4]
ZnFe ₂ O ₄ nanoparticles	~68	~615/50/60		[5]
ZnFe ₂ O ₄ /C hollow spheres	~67	~841/30/65		[6]
ZnFe ₂ O ₄ nano-octahedrons	~77	~730/300/1000		[7]
ZnFe ₂ O ₄ /graphene	~64	~398/90/400		[8]
ZnFe ₂ O ₄ hollow microspheres	~71	~584/100/100		[9]
ZnFe ₂ O ₄ /graphene	~68.6	~956/50/100		[10]
Nano-ZnFe ₂ O ₄	~69	~833/50/116		[11]
ZnO/ZnFe ₂ O ₄ microcubes	sub-	~837/200/1000		[12]
ZnFe ₂ O ₄ /graphene	~69	~464/300/800		[13]

- [1] J. M. Won, S. H. Choi, Y. J. Hong, Y. N. Ko, Y. C. Kang, *Sci. Rep.* **2014**, 4, 4857.
- [2] L. Lin, Q. M. Pan, *J. Mater. Chem. A* **2015**, 3, 1724.
- [3] R. M. Thankachan, M. M. Rahman, I. Sultana, A. M. Glushenkov, S. Thomas, N. Kalarikkal, Y. Chen, *J. Power Sources* **2015**, 282, 462.
- [4] P. F. The, Y. Sharma, S. S. Pramana, M. Srinivasan, *J. Mater. Chem.* **2011**, 21, 14999.
- [5] Y. Sharma, N. Sharma, G. V. S. Rao, B. V. R. Chowdari, *Electrochim. Acta* **2008**, 53, 2380.
- [6] Y. F. Deng, Q. M. Zhang, S. D. Tang, L. T. Zhang, S. N. Deng, Z. C. Shi, G. H. Chen, *Chem. Commun.* **2011**, 47, 6828.
- [7] Z. Xing, Z. C. Ju, J. Yang, H. Y. Xu, Y. T. Qian, *Nano Res.* **2012**, 5, 477.
- [8] W. T. Song, J. Xie, S. Y. Liu, G. S. Cao, T. J. Zhu, X. B. Zhao, *New J. Chem.* **2012**, 36, 2236.
- [9] L. M. Yao, X. H. Hou, S. J. Hu, Q. Ru, X. Q. Tang, L. Z. Zhao, D. W. Sun, *J. Solid State Electrochem.* **2013**, 17, 2055.
- [10] H. Xia, Y. Y. Qian, Y. S. Fu, X. Wang, *Solid State Sci.* **2013**, 17, 67.
- [11] Y. Ding, Y. F. Yang, H. X. Shao, *Electrochim. Acta* **2011**, 56, 9433.
- [12] L. R. Hou, L. Lian, L. H. Zhang, G. Pang, C. Z. Yuan, X. G. Zhang, *Adv. Funct. Mater.* **2015**, 25, 238.
- [13] J. Xie, W. T. Song, G. S. Cao, T. J. Zhu, X. B. Zhao, S. C. Zhang, *RSC Adv.* **2014**, 4, 7703.

Table S4 Fitted results from the Nyquist plots (**Fig. S10**) for the ZZFO and ZZFO@C anodes, respectively

Samples	R _s (Ohm)	R _{CT} (Ohm)
ZZFO	~5.1	~287
ZZFO@C	~2.5	~176